Localized buckling of a microtubule surrounded by randomly distributed cross linkers

M. Z. Jin and C. Q. Ru*

Department of Mechanical Engineering, University of Alberta, Edmonton, Canada T6G 2G8

(Received 15 November 2012; revised manuscript received 26 April 2013; published 3 July 2013)

Microtubules supported by surrounding cross linkers in eukaryotic cells can bear a much higher compressive force than free-standing microtubules. Different from some previous studies, which treated the surroundings as a continuum elastic foundation or elastic medium, the present paper develops a micromechanics numerical model to examine the role of randomly distributed discrete cross linkers in the buckling of compressed microtubules. First, the proposed numerical approach is validated by reproducing the uniform multiwave buckling mode predicted by the existing elastic-foundation model. For more realistic buckling of microtubules surrounded by randomly distributed cross linkers, the present numerical model predicts that the buckling mode is localized at one end in agreement with some known experimental observations. In particular, the critical force for localized buckling, predicted by the present model, is insensitive to microtubule length and can be about 1 order of magnitude lower than those given by the elastic-foundation model, which suggests that the elastic-foundation model may have overestimated the critical force for buckling of microtubules *in vivo*. In addition, unlike the elastic-foundation model, the present model can capture the effect of end conditions on the critical force and wavelength of localized buckling. Based on the known data of spacing and elastic constants of cross linkers available in literature, the critical force and wavelength of the localized buckling mode, predicted by the present model, are compared to some experimental data with reasonable agreement. Finally, two empirical formulas are proposed for the critical force and wavelength of the localized buckling of microtubules surrounded by cross linkers.

DOI: 10.1103/PhysRevE.88.012701 PACS number(s): 87.17.Rt, 87.17.Aa

I. INTRODUCTION

The microtubule is one of the most important cytoskeletal elements in eukaryotic cells [1]. Although mechanical behaviors of microtubules *in vitro* were well predicted by the elastic column model, microtubules *in vivo* (typically tens of microns in length) can bear a much higher compressive force than that *in vitro*. The increase in critical buckling force is attributed to surrounding cross linkers, which are often modeled as a continuous and homogenous elastic foundation [2–4]. As a result of the lateral elastic constraint, the multiwave buckling mode charactzerized by uniform short buckling waves with smaller deflection is energically favorable over the single-wave buckling mode predicted by the free-standing elastic column model. With such an elastic-foundation model, the critical compressive force and associated wavelength of the buckling modes can be calculated by the conventional method of elastic buckling [5]. In particular, the predicted critical force and wavelength are insensitive to the length of the microtubules and the end conditions.

Despite the success of the elastic-foundation model in explaining the higher critical buckling force, this model suffers several limitations. First, the relationship between the elastic-foundation modulus and the properties of discrete cross linkers remains a problem to be addressed [3,6–9]. Actually, the commonly used approach to determine the elastic-foundation modulus is under the assumption of in-plane two dimensional (2D) buckling [5], which is inappropriate for the three dimensional (3D) microtubule cross linker system. More importantly, refereed as "localized buckling" by some authors (see, e.g., Brangwynne *et al.* [2]), microtubule buckling *in vivo* exhibits a localized buckling mode in which the magnitude of deflection quickly decays from the site where the compressive force is applied. Similar localized buckling modes are observed in other experiments [10,11]. The observed localized buckling is inconsistent with the uniform multiwave buckling mode predicted by the elastic-foundation model [3,8,9]. In addition, the possible effect of end conditions (e.g., free or clamped), which may lead to different buckling wavelengths and critical forces, cannot be captured by the elastic-foundation model. In view of the fact that the critical force for observed localized buckling could be much lower than that given by the elastic-foundation model based on the uniform multiwave buckling mode, this discrepancy deserves further study. To this end, it is crucial to examine the role of discrete cross linkers *in vivo,* which are laterally attached to microtubules and are distributed randomly in both longitudinal and circumferential directions [1]. Furthermore, as suggested by the "tensegrity" model [12,13], the cross linkers have negligible bending rigidity and cannot bear compressive force, a feature which cannot be well modeled by the existing elastic-foundation model.

In the present paper, a micromechanics numerical model is developed to simulate buckling behavior of microtubules based on the measured properties and observed morphology of microtubules and cross linkers. The proposed numerical model is validated by comparing its predictions with the elastic-foundation model for simple 2D in-plane buckling of a microtubule supported by continuously distributed linear springs. The validated model is then employed to investigate 3D buckling behaviors of the microtubule cross linker system. Based on our numerical simulations, two empirical relations are proposed for the critical force and wavelength of the localized buckling of microtubules. As will be shown in the paper, the localized buckling of microtubules, predicted by the present model, is in reasonable agreement with some recent experimental data.

*Corresponding author: cru@ualberta.ca

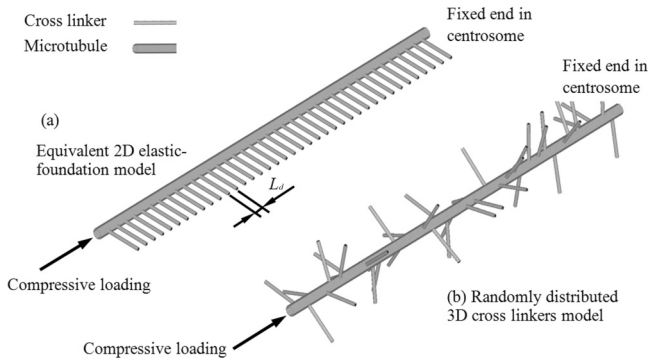

FIG. 1. The present numerical models: (a) equivalent 2D elastic-foundation model; (b) randomly distributed 3D cross linkers model.

II. THE MICROMECHANICS NUMERICAL MODEL

The microtubule cross linker system, studied in the present paper, is composed of a microtubule surrounded by cross linkers randomly distributed along the longitudinal direction, see Fig. 1. The microtubule is modeled as an elastic hollow cylinder column as presented in Sec. II A, whereas, the modeling of cross linkers is illustrated in Secs. II B1 and II B2. The two key parameters of the cross linkers are the spring constant k and the spacing of cross linkers L_d, whose values will be given based on available experimental data. Buckling of microtubules is stimulated by imposing compressive axial displacement at one end of the microtubule with the other end fixed.

A. Microtubule modeling

The microtubule is modeled as a hollow cylinder column with an outer diameter of 25 nm and a thickness of 1.86 nm [9,14]. The geometry of the cross section and Young's modulus E of 1 GPa [15] give the bending rigidity EI of 9.034×10^{-24} Nm^2, which is within the range of the measured values of several experiments [16]. The length of microtubule L in the present study is between 300 nm, which is almost the minimum length of the microtubules in experiments [17], and a few tens of microns. As our major concern is the localized mode or uniform multiwave buckling mode with a shorter wavelength (typically, around 1–3 μm), the length dependency of bending rigidity [18] is not included in the present paper. Thus, the 3D Timoshenko shear deformable beam elements are used to mesh the microtubule. The microtubule is always clamped on one end as it is anchored in the centrosome in living cells [1,17]. Another end of the microtubule is subjected to a compressive load under different types of end conditions (e.g., free or clamped) [1]. To initiate the buckling of the microtubule, an extremely small perturbation force is applied at the end in the direction perpendicular to the microtubule. Our simulations show that the magnitude of the small perturbation force is irrelevant to simulation results.

B. Modeling of cross linkers

All cross linkers are modeled as linear springs with one end permanently attached to the microtubule and the other end fixed in all degrees of freedom. The spring constant k of the cross linkers (of length 45 nm) used here, 39 pN/nm, is taken from Ref. [19]. As the spring constant k may change for different types of cross linkers, a wider range of the spring constant (which may depend on the length of the cross linkers) is also considered in the present paper. On the other hand, the spacing L_d ranging from 25 to 300 nm [19,20] will be considered. The 3D elastic linear spring elements are used to mesh the cross linkers. Two numerical models, characterized by different distributions and constitutive laws of cross linkers, are illustrated below, referred to as the equivalent elastic-foundation model and the randomly distributed 3D cross linker model, respectively.

1. Equivalent elastic-foundation model

To demonstrate the efficiency of the present numerical model, first, we will apply it to the simple 2D in-plane uniform multiwave buckling and compare its results with the elastic-foundation model. For the 2D in-plane buckling of a microtubule supported by a continuum elastic foundation, the wavelength and critical buckling force are given by [4]

$$\lambda = 2\pi \left(\frac{EI}{E_c} \right)^{1/4}, \tag{1}$$

and

$$F_{\mathrm{cr}} = 2\sqrt{E_c EI} = 8\pi^2 \frac{EI}{\lambda^2}, \tag{2}$$

where EI is the bending rigidity of the microtubule and E_c is the elastic-foundation modulus. The elastic-foundation modulus E_c in the 2D condition is directly proportional to the spring constant k and is inversely proportional to the spacing L_d of the uniformly distributed linear springs [5] as

$$E_c = \frac{k}{L_d}. \tag{3}$$

This formula (3) is commonly used provided that L_d is much smaller than the wavelength.

To compare the present numerical model with the elastic-foundation model, a 2D numerical model is shown in Fig. 1(a) where all cross linkers are aligned on the same plane and are perpendicular to the microtubule. All out-of-plane displacements and rotations are not allowed. In addition, as assumed in the elastic-foundation model, all cross linkers in the equivalent elastic-foundation model shown in Fig. 1(a) are capable of bearing both compressive and tensile forces [12,13].

2. Randomly distributed 3D cross linker model

The major goal of the present study is buckling behaviors of a microtubule surrounded by 3D randomly distributed discrete cross linkers. The morphological details of the cross linkers are modeled based on experimental observations. All cross linkers are attached to the microtubule in random directions assigned by the uniform distribution rule, see Fig. 1(b). The cross linkers are modeled as linear springs with negligible bending rigidity [9,21], thus, they can bear axial tension but are vulnerable to any axial compression. To realize this, the load increments are sufficiently small, and every spring element is verified after each load increment and will be permanently removed if the axial force becomes compressive (actually, if a small nonzero threshold value of compressive force, such as 1 to 2 pN, is

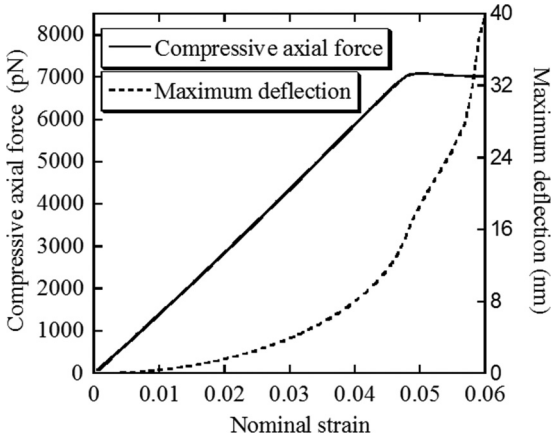

FIG. 2. A typical relation between the compressive axial force or the maximum deflection and the nominal axial strain given by the present model.

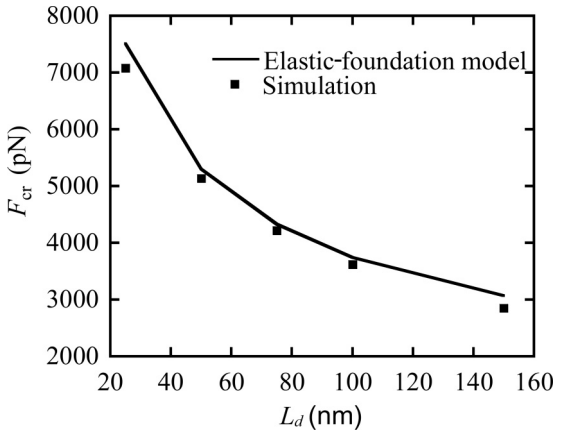

FIG. 3. Critical buckling forces F_{cr} predicted by the present equivalent elastic-foundation model compared with the elastic-foundation formulas Eqs. (1) and (2) with $k = 39$ pN/nm.

used, our results remain essentially unchanged. Therefore, we have simply set the threshold value as zero). Different from the equivalent elastic-foundation model described in Sec. II B 1 (where out-of-plane displacements and rotations are not allowed), the 3D buckling behaviors are modeled by allowing buckling deflections in all directions.

III. NUMERICAL RESULTS AND TWO EMPIRICAL RELATIONS

In all numerical simulations presented in this section, the applied axial displacement is given in terms of the dimensionless nominal axial strain (defined by the ratio of the applied axial displacement to the length of the microtubule), and the associated axial force (in piconewtons) is calculated based on the deflected equilibrium state of the microtubule. The axial force at the node where the axial compressive displacement is applied is defined as the axial compressive force applied to the microtubule.

A. Classical uniform multiwave buckling mode

First, let us consider the classic 2D uniform multiwave buckling mode, which evenly spreads over the entire microtubule [5]. In this case, the results given by the present equivalent elastic-foundation model are compared with the classical elastic-foundation model.

First, compared are the critical buckling forces predicted by the present numerical model and the classical formula Eq. (2). From the present numerical model, a curve of the axial compressive force versus the nominal axial strain is plotted in Fig. 2 with $k = 39$ pN/nm and $L_d = 25$ nm. From Fig. 2, it is seen that the axial compressive force linearly increases with the nominal axial strain until a plateau is reached. Also included in Fig. 2 is the maximum deflection of the microtubule, which upturns remarkably as the plateau is approached. Therefore, the critical buckling force F_{cr} from our numerical simulations is defined as the axial compressive force on the plateau. From Fig. 2, it is seen that, after the critical force is reached, the axial compressive strain increases quickly without significant change in the axial force (for example, the axial force changes only by less than 5% as the axial strain doubles). From Fig. 3, it is seen that the critical buckling force F_{cr}, given by the present numerical model, is in good agreement with Eq. (2). In particular, consistent with the elastic-foundation model, the critical buckling force predicted by the present numerical model is insensitive to the microtubule length.

Three buckling modes given by our numerical models are shown in Fig. 4 with a good comparison to the classical wavelength formulas Eqs. (1) and (3). In Fig. 4(a), the shorter wavelength is associated with the highest spring constant $k = 39$ pN/nm and the shortest spacing $L_d = 25$ nm. In particular, our numerical results confirm that the buckling predicted by the 2D equivalent elastic-foundation model is characterized by the uniform multiwave mode rather than the localized mode, and the predicted wavelength is insensitive to the length of the microtubule.

B. Localized buckling mode

Now, let us investigate 3D buckling behaviors of the microtubule cross linker system using the randomly distributed 3D cross linkers model. From Fig. 5, it is seen that a remarkable feature of the buckling behavior given by our 3D cross linkers model is that the buckling mode is highly localized near the end, which bears great similarity with the microtubule buckling observed *in vivo* by Brangwynne *et al.* [2] and refereed as localized buckling. Although the localized buckling mode, obtained in our simulations, is actually 3D in nature, the out-of-plane helical deflection is much smaller than the in-plane deflection. Here, it should be noted that the localized buckling mode, predicted by the present static 3D cross linkers model, is significantly different from those reported in some previous papers, say, the localized mode caused by the wave of compressive force propagating from one end at which the localized buckling mode is initiated [22] or the localized mode as a result of the large deflection postbuckling of a compressed column on a 2D elastic foundation [23,24], which has the uniform multiwave mode as its linearized buckling mode. Different than these mentioned papers, the localized mode, obtained by the present model, is static in nature and is not a result of postbuckling developed from an initial uniform multiwave buckling mode.

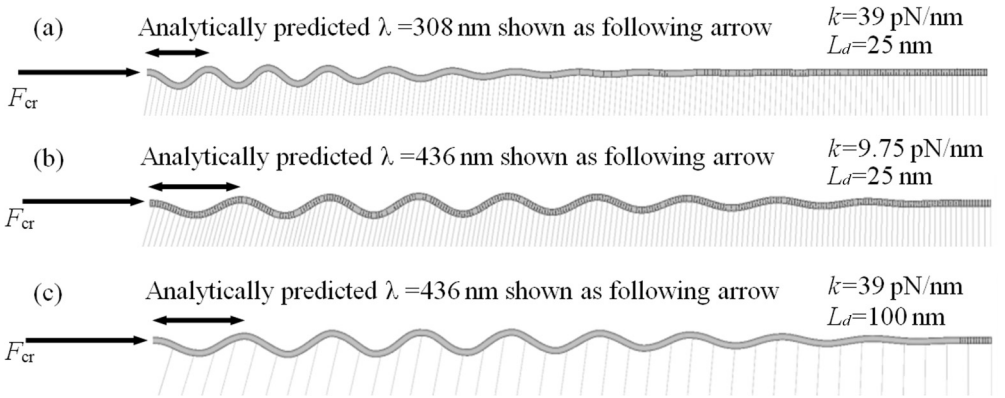

FIG. 4. Two-dimensional in-plane multiwave buckling modes (buckled gray color beam) given by the present equivalent elastic-foundation model compared with the wavelengths given by the classical elastic-foundation model Eq. (1) (black arrows).

What is shown in Fig. 5 is the dependence of the critical buckling force F_{cr} on the microtubule length. Although the critical buckling force F_{cr} changes considerably with length for extremely short microtubules (say, F_{cr} decreases from 511 to 365 pN as the length of the microtubule increases from 300 to 500 nm), the critical force F_{cr} becomes length independent when the microtubule length exceeds a critical value (say, larger than 500 nm). For example, for a microtubule of 2000 nm in length, the critical force F_{cr} for localized buckling is around 360 pN (which is almost the same as the critical force of 365 pN for a microtubule of 500 nm in length), and the localized buckling wavelength is about 500 nm (almost the same as the localized buckling wavelengths of much shorter microtubules). In Fig. 6, it can be seen how the buckling force F_{cr} quickly converges to a constant, defined as the localized critical buckling force F_L, when the length of microtubule exceeds a critical value (say, 500 nm for $k = 39$ pN/nm and $L_d = 50$ nm). Indeed, the critical force F_L for localized buckling and the associated wavelength λ_L become essentially length independent when the microtubule length exceeds a critical value.

The spring constant k and spacing L_d of the cross linkers influence the predicted critical force F_L and wavelength λ_L of localized buckling as well as the critical length of microtubules beyond which F_L and λ_L become essentially length independent. For example, our numerical results show that, as spacing L_d changes from 25 to 100 nm with $k =$ 39 pN/nm, the critical length of the microtubules, beyond which F_L and λ_L essentially keep constant, increases with the increasing spacing L_d. Additionally, as expected, our simulations show that a higher critical force F_L and a shorter wavelength λ_L are achieved with a larger spring constant of cross linkers as detailed in Sec. III C.

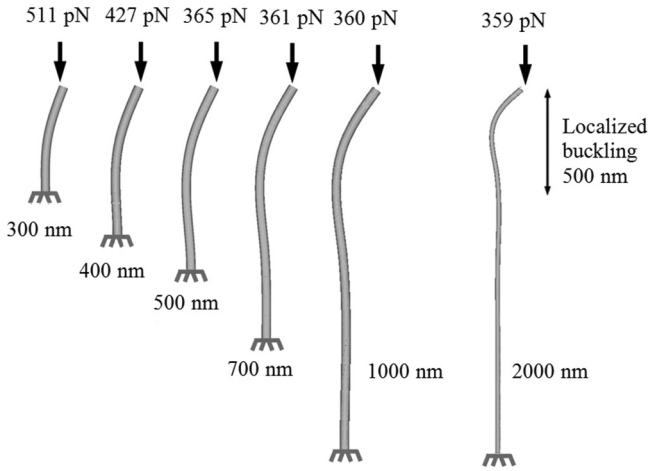

FIG. 5. Buckling of a microtubule given by the present randomly distributed 3D cross linkers model with spring constant $k =$ 39 pN/nm and spacing $L_d = 50$ nm. The buckling wavelength and critical buckling force are essentially length independent as the length of the microtubule is much longer than the buckling wavelength.

C. Two empirical relations for localized buckling

The localized buckling is characterized by the two key parameters, the localized buckling wavelength λ_L and the

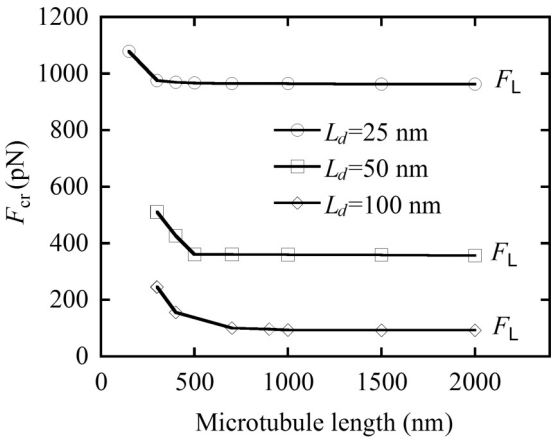

FIG. 6. The critical force F_{cr} quickly converges to a constant (defined as the localized buckling force F_L) as the microtubule length exceeds a critical length (the latter is around 500 nm when $L_d =$ 50 nm). This critical length increases with increasing spacing of cross linkers L_d. The critical force F_{cr} quickly converges to a constant (defined as the localized buckling force F_L) as the microtubule length exceeds a critical length (the latter is around 500 nm when L_d). This critical length increases with increasing spacing of cross linkers L_d .

critical force F_L for localized buckling. In what follows, based on our numerical simulations, two empirical relations will be given for the dependency of the two key parameters on the spring constant k and the spacing L_d of the cross linkers.

In view of the classical formula (1), we seek an empirical relation for the localized buckling wavelength of the following form:

$$\lambda = 2\pi \left(\frac{EI}{A}\right)^{1/4} \left(\frac{k_0}{k}\right)^{p/4} \left(\frac{L_d}{L_0}\right)^{q/4}, \tag{4}$$

where A, p, and q will be determined to fit numerical data (A is measured in pascals, whereas, p and q are dimensionless). The reference spacing L_0 is 25 nm (which is probably the shortest cross linker spacing, say with the length of guanosine 5′-triphosphate/guanosine 5′-diphosphate dimers of 8.1 nm, see Ref. [25]), and the reference spring constant of cross linkers k_0 is 39 pN/nm [19]. In view of the classical formula (2), we also seek an empirical relation for the critical force for the localized buckling of the following form:

$$F_L = \frac{B\pi^2}{4}\frac{EI}{\lambda_L^2} = \frac{B}{16}\sqrt{EIA}\left(\frac{k}{k_0}\right)^{p/2}\left(\frac{L_0}{L_d}\right)^{q/2}, \tag{5}$$

where B is a dimensionless constant. To determine p and q, based on our numerical simulations, we rewrite Eq. (5) as

$$\ln F_L = \ln\left[\frac{B}{16}\sqrt{EIA}\left(\frac{L_0}{L_d}\right)^{q/2}\right] + \frac{p}{2}\ln\left(\frac{k}{k_0}\right), \tag{6}$$

and

$$\ln F_L = \ln\left[\frac{B}{16}\sqrt{EIA}\left(\frac{k}{k_0}\right)^{p/2}\right] + \frac{q}{2}\ln\left(\frac{L_0}{L_d}\right). \tag{7}$$

In Eqs. (6) and (7), $p/2$ and $q/2$ are the slopes of the curves of $\ln F_L$ versus $\ln(k/k_0)$ and $\ln(L_0/L_d)$, respectively. The simulation results with different combinations of k and L_d are linearly fitted in Figs. 7(a) and 7(b), which gives q and p as 3.6 and 0.47, respectively. With the values of q, p, and the wavelengths given by our simulations, the value of A is determined as 1.4 MPa from Eq. (4). With all of these values obtained, the constant B is obtained as 5.3 from Fig. 7(a) and Eq. (6). Finally, two empirical relations for the critical force and the associated wavelength for the localized buckling are given as

$$\lambda_L = 2\pi\left(\frac{EI}{1.4\ \text{MPa}}\right)^{1/4}\left(\frac{k_0}{k}\right)^{0.12}\left(\frac{L_d}{L_0}\right)^{0.90}, \tag{8}$$

and

$$F_L = 1.3\pi^2\frac{EI}{\lambda_L^2}. \tag{9}$$

Since p and q are determined using the data of critical force F_L given by Eq. (5), the predicted wavelength λ_L from Eq. (8) is further compared with the data obtained directly from simulations. Again, good agreement is achieved for $k = k_0$, $k_0/4$, $k_0/16$, $k_0/32$, and $k_0/64$ as shown in Fig. 8. Validity of the proposed relations (8) and (9) is also verified for different values of bending rigidities EI. For example, in a series of experiments by Felgner *et al.* [26], the bending rigidity of the microtubule was measured as low as 3.8×10^{-24} Nm^2 [26]. With the bending rigidity EI of 3.8×10^{-24} Nm^2 and the other

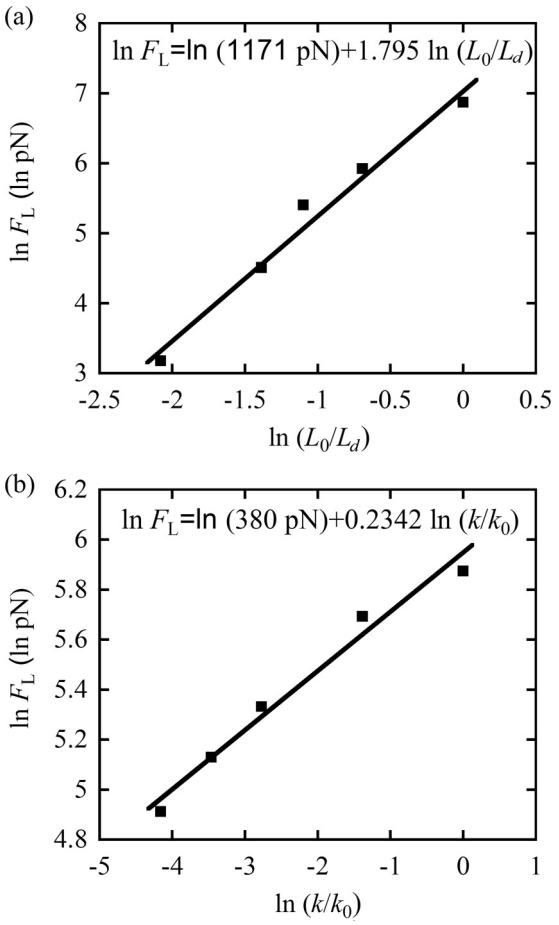

FIG. 7. Determination of p and q in the proposed empirical equations (5) by linearly fitting simulation results of the localized buckling.

parameters adopted in Fig. 5, the critical buckling force given by the empirical formula Eq. (9) is 218 pN, which is reasonably close to 234 pN obtained by direct numerical simulations with $EI = 3.8 \times 10^{-24}$ Nm^2. The two empirical relations (8) and (9) are expected to be useful within a reasonable range of the spring constant (from $k_0/64$ to k_0) and the spacing (from 25 to 300 nm) of the cross linkers and under the condition that the

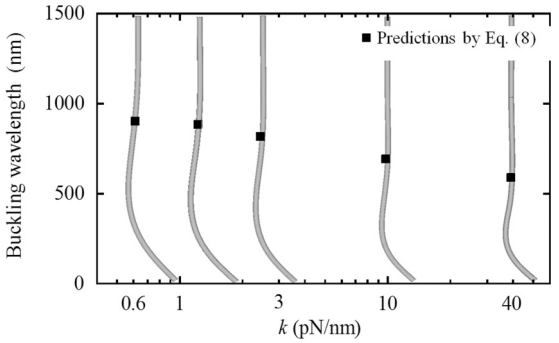

FIG. 8. Localized buckling wavelength λ_L given by the present numerical model compared with the wavelength calculated from the empirical equation (8).

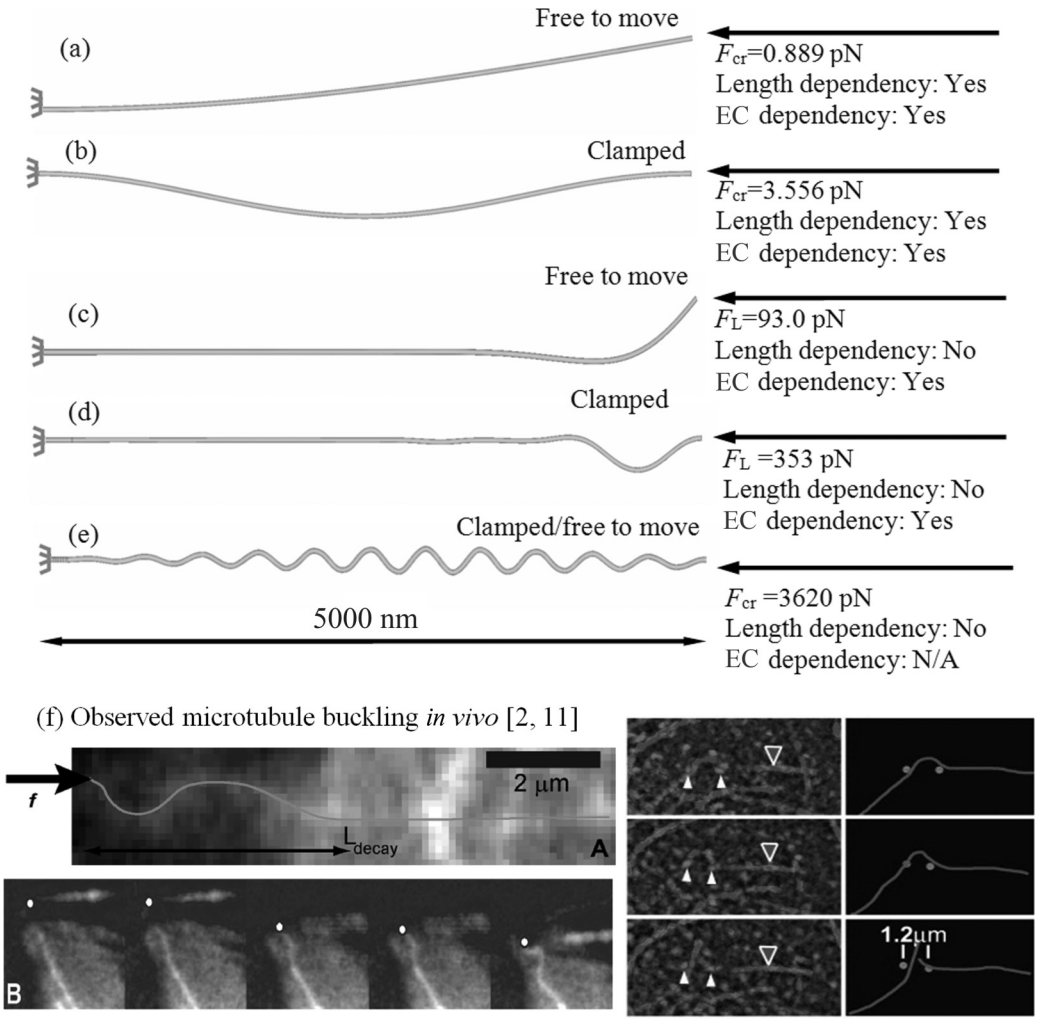

FIG. 9. Different buckling cases with different end conditions (ECs) of microtubule *in vivo/in vitro*: the free-standing microtubule buckling with (a) clamped-free or (b) clamped-clamped end conditions observed *in vitro* [27,28]; (c) the localized buckling with clamped-free and (d) doubly clamped end conditions, which are similar to the observation *in vivo* [2,10,11], see (f); and (e) the multiwave buckling mode obtained by the equivalent elastic-foundation model. ©2006 Rockefeller University Press, J. Cell Biol. and 2002 Elsevier, Curr. Biol.

localized buckling wavelength λ_L is, at least, ten times longer than the spacing L_d.

The proposed empirical formulas (8) and (9), obtained by fitting with our numerical data, are significantly different than the 2D elastic-foundation formulas (1) and (2). For example, the critical force for the localized buckling predicted by Eq. (9) is about 1/6 of the buckling force predicted by the elastic-foundation model (2) based on the same buckling wavelength, which indicates that the critical buckling force of the localized buckling is much lower than that predicted by the elastic-foundation model based on the in-plane uniform multiwave buckling mode. In addition, although both our empirical formulas (8) and (9) and 2D elastic-foundation formulas (1) and (2) predict that the critical buckling force increases with the spring constant k and decreases with the spacing L_d, the dependence of the critical buckling force on the spring constant k decreases from the power index of 0.5 in the 2D model to 0.22 in our 3D model, and the dependence of the critical buckling force on the spacing L_d increases from the power index of 0.5 in the 2D model to 1.8 in our 3D model.

IV. COMPARISON WITH KNOWN EXPERIMENTAL RESULTS

Let us now compare the results of localized buckling given by the present model with some known experimental measurements as well as the elastic-foundation model and the free-standing elastic column model. In what follows, the microtubules in all cases are of the common length of 5 μm, which guarantees that the wavelengths of the localized buckling mode and the uniform multiwave buckling mode are much shorter than the length of the microtubule.

The buckling modes given by the three models, shown in Fig. 9, are significantly different. The buckling of a free-standing microtubule under the free or clamped end condition is illustrated in Figs. 9(a) and 9(b), respectively. With

$L_d = 100$ nm and $k = 39$ pN/nm, the localized buckling, given by the present model under the free or clamped end condition, is shown in Figs. 9(c) and 9(d), respectively. Finally, the buckling mode and the critical buckling force of the uniform multiwave buckling, given by the equivalent elastic-foundation model (described in Sec. II B 1), is presented in Fig. 9(e) with the same L_d and k as adopted in Figs. 9(c) and 9(d). All predicted buckling behaviors are compared with experimental observations [2,10,11] shown in Fig. 9(f).

The localized buckling modes, given by the present model in Figs. 9(c) and 9(d) with two different end conditions, bear a resemblance to the observed microtubule buckling mode *in vivo* shown in Fig. 9(f) [2,10,11]. Although the actual end conditions of the microtubules *in vivo* [2,10,11] are uncertain, all observed buckling modes are localized in nature, which are consistent with our simulations shown in Figs. 9(c) and 9(d) but cannot be explained by the 2D elastic-foundation model. On the other hand, the single-wave buckling mode given by the free-standing microtubule model is only comparable with *in vitro* experiments [27,28] but fails to predict the buckling behaviors of the microtubules surrounded by the cross linkers in living cells.

Also, the present model can effectively predict the critical force for localized buckling and the associated buckling wavelength. For example, with $L_d = 100$ nm and $k = 39$ pN/nm [19,20], the localized buckling wavelength and critical force, given by the present numerical model under a free end condition in Fig. 9(c), are about 1.2 μm and 93 pN, respectively, similar results of 1.10 μm and 97.3 pN can be obtained from the empirical Eqs. (8) and (9). With the clamped end condition in Fig. 9(d), on the other hand, the localized buckling wavelength and critical force, given by the present model, are about 1 μm and 353 pN, respectively. The two predicted wavelengths reasonably agree with the observed wavelength around 1 to 2 μm shown in Fig. 9(f). With a slightly different spring constant and spacing of the cross linkers, the predicted buckling wavelengths still fall into the range of experimental measurements, say 1–3 μm [2,10,11]. For example, the longer buckling wavelength of 3 μm can be obtained by the present model with the spacing of 300 nm [29]. In addition, the critical forces for the localized buckling, predicted by the present model as 93.0 or 353 pN, are also in reasonable agreement with the well-recognized concept that the critical buckling force of microtubules *in vivo* would be around 100 pN [2,8,30].

Clearly, if the free-standing column model or the elastic-foundation model is adopted with the above data of spring constants and spacing of cross linkers, the predicted critical buckling force and wavelength are different from experimental measurements by almost 1 order of magnitude. For example, the critical buckling forces, predicted by the free-standing column model, are only 0.889 and 3.556 pN for a free or clamped end. On the other hand, if the elastic-foundation model is adopted with the foundation modulus given by Eq. (3) with the same data of cross linkers as those used in Figs. 9(c) and 9(d), the predicted buckling wavelength, about 400 nm, is much shorter than the measured buckling wavelength. Actually, in order to predict the measured buckling wavelength of 2 to 3 μm with the bending rigidity of the microtubules adopted in Refs. [2,4], i.e., 20×10^{-24} Nm^2 and $L_d = 100$ nm, the elastic-foundation model requests a spring constant of cross linkers k as low as 0.078 pN/nm, which is much lower than the spring constant of most types of protein polymers attached to microtubules (e.g., the actin filaments, 1 μm in length, have the spring constant of 44 pN/nm [17], and tau protein, which links microtubules to form bundles, has the spring constant of 39 pN/nm [19]) and is almost 1 order of magnitude lower than the lower limit of the measured lower limit of kinesin (i.e., 0.65−1.7 pN/nm) [31], a key motor protein attached to microtubules for cellular transportation. Therefore, although the elastic-foundation model could also give the measured buckling wavelength, the assumed elastic-foundation modulus [3,6,8] cannot be obtained through Eq. (3) from the known data of cross linkers reported in literature [19,20,29]. Thus, it seems reasonable to conclude that, as compared with the elastic-foundation model, the present discrete cross linkers model can better explain the observed wavelength and critical force of the localized buckling of microtubules in living cells.

Physically, for a number of reasons, we also believe that the present 3D discrete numerical model can better capture realistic conditions for microtubules in living cells as compared with the 2D elastic-foundation model. First, the cross linkers in living cells are discrete and 3D in nature, which cannot be appropriately described by the 2D continuum elastic-foundation model. Second, the geometrical nonlinearity, which is included in the present numerical model, cannot be easily carried out by the classic linear buckling analysis. Third, the cross linkers cannot be idealized as a linear elastic foundation because they cannot bear compressive force due to very low bending rigidity, a feature captured in the present 3D discrete numerical model.

V. CONCLUSIONS

A numerical micromechanics model is proposed to investigate the axially compressed buckling of a microtubule surrounded by randomly distributed discrete cross linkers. The localized buckling behavior observed *in vivo* [2,10,11], which cannot be predicted by the existing models, is well explained by the present numerical model. Based on our numerical simulations, two empirical relations are proposed to calculate the critical force and associated wavelength of the localized buckling. For typical cross linkers of the spacing of 50–300 nm and the spring constant of 39 pN/nm as reported in literature [19,20,29], the present model predicts that microtubules could buckle under an axial compressive force of about 14–340 pN with a localized buckling mode of wavelengths of 0.6–2.9 microns, in reasonable agreement with a few recent experiments [2,8,30].

ACKNOWLEDGMENTS

The authors gratefully acknowledge the financial support of the Natural Science and Engineering Research Council (NSERC) of Canada through Grant No. RGPIN 204992 and Alberta Innovates Graduate Student Scholarship of the University of Alberta.

[1] D. Boal, *Mechanics of the Cell* (Cambridge University Press, Cambridge, UK, 2002).
[2] C. P. Brangwynne, F. C. MacKintosh, S. Kumar, N. A. Geisse, J. Talbot, L. Mahadevan, K. K. Parker, D. E. Ingber, and D. A. Weitz, J. Cell Biol. **173**, 733 (2006).
[3] H. Q. Jiang and J. P. Zhang, J. Appl. Mech. **75**, 061019 (2008).
[4] G. W. Brodland and R. Gordon, J. Biomech. Eng. **112**, 319 (1990).
[5] A. C. Ugural and S. K. Fenster, *Advanced Strength and Applied Elasticity* (Prentice Hall, Upper Saddle River, NJ, 2003).
[6] C. Wang, C. Li, and S. Adhikari, J. Biomech. **42**, 1270 (2009).
[7] Y. Gao and L. An, Physica E (Amsterdam) **42**, 2406 (2010).
[8] T. Li, J. Biomech. **41**, 1722 (2008).
[9] M. Mehrbod and M. R. K. Mofrad, PloS One **6**, e25627 (2011).
[10] C. A. Mandato and W. M. Bement, Curr. Biol. **13**, 1096 (2003).
[11] S. L. Gupton, W. C. Salmon, and C. M. Waterman-Storer, Curr. Biol. **12**, 1891 (2002).
[12] N. Wang, K. Naruse, D. Stamenovic, J. J. Fredberg, S. M. Mijailovich, I. M. Toric-Norrelykke, T. Polte, R. Mannix, and D. E. Ingber, Proc. Natl. Acad. Sci. USA **98**, 7765 (2001).
[13] P. Canadas, V. M. Laurent, C. Oddou, D. Isabey, and S. Wendling, J. Theor. Biol. **218**, 155 (2002).
[14] M. Z. Jin and C. Q. Ru, J. Appl. Phys. **111**, 064701 (2012).
[15] C. Li, C. Q. Ru, and A. Mioduchowski, Biochem. Biophys. Res. Commun. **349**, 1145 (2006).
[16] T. Hawkins, M. Mirigian, M. Selcuk Yasar, and J. Ross, J. Biomech. **43**, 23 (2010).
[17] J. Howard, *Mechanics of Motor Proteins and the Cytoskeleton* (Sinauer Associates, Inc., Sunderland, MA, 2001).
[18] F. Pampaloni, G. Lattanzi, A. Jonáš, T. Surrey, E. Frey, and E. L. Florin, Proc. Natl. Acad. Sci. USA **103**, 10248 (2006).
[19] S. J. Peter and M. R. K. Mofrad, Biophys. J. **102**, 749 (2012).
[20] T. M. Svitkina, A. B. Verkhovsky, and G. G. Borisy, J. Cell Biol. **135**, 991 (1996).
[21] M. Bathe, C. Heussinger, M. M. A. E. Claaessens, A. R. Bausch, and E. Frey, Biophys. J. **94**, 2955 (2008).
[22] P. Ranjith and P. B. S. Kumar, Phys. Rev. Lett. **89**, 018302 (2002).
[23] G. W. Hunt, M. K. Wadee, and N. Shiacolas, J. Appl. Mech. **60**, 1033 (1993).
[24] S. H. Lee and A. M. Waas, Int. J. Non-Linear Mech. **31**, 313 (1996).
[25] V. Hunyadi, D. Chrétien, H. Flyvbjerg, and I. Janosi, Biol. Cell **99**, 117 (2007).
[26] H. Felgner, R. Frank, J. Biernat, E. M. Mandelkow, E. Mandelkow, B. Ludin, A. Matus, and M. Schliwa, J. Cell Biol. **138**, 1067 (1997).
[27] M. Kikumoto, M. Kurachi, V. Tosa, and H. Tashiro, Biophys. J. **90**, 1687 (2006).
[28] M. Elbaum, D. K. Fygenson, and A. Libchaber, Phys. Rev. Lett. **76**, 4078 (1996).
[29] L. M. Griffith and T. D. Pollard, J. Cell Biol. **78**, 958 (1978).
[30] F. Gittes, B. Mickey, J. Nettleton, and J. Howard, J. Cell Biol. **120**, 923 (1993).
[31] N. J. Carter and R. A. Cross, Nature (London) **435**, 308 (2005).